

High performance and cost effective CO-OFDM system aided by polar code

LING LIU,¹ SHILIN XIAO,^{1,*} JIAFEI FANG,¹ LU ZHANG,¹ YUNHAO ZHANG,¹ MEIHUA BI,^{1,2} AND WEISHENG HU¹

¹State Key Laboratory of Advanced Optical Communication System and Networks, Department of Electronic Engineering, Shanghai Jiao Tong University, Shanghai 200240, China

²College of Communication Engineering, Hangzhou Dianzi University, Xiasha Gaojiaoyuan 2nd Street, Hangzhou, Zhe Jiang Province, 310018, China

*slxiao@sjtu.edu.cn

Abstract: A novel polar coded coherent optical orthogonal frequency division multiplexing (CO-OFDM) system is proposed and demonstrated through experiment for the first time. The principle of a polar coded CO-OFDM signal is illustrated theoretically and the suitable polar decoding method is discussed. Results show that the polar coded CO-OFDM signal achieves a net coding gain (NCG) of more than 10 dB at bit error rate (BER) of 10^{-3} over 25-Gb/s 480-km transmission in comparison with conventional CO-OFDM. Also, compared to the 25-Gb/s low-density parity-check (LDPC) coded CO-OFDM 160-km system, the polar code provides a NCG of 0.88 dB @BER = 10^{-3} . Moreover, the polar code can relieve the laser linewidth requirement massively to get a more cost-effective CO-OFDM system.

© 2017 Optical Society of America

OCIS codes: (060.2330) Fiber optics communications; (060.1660) Coherent communications.

References and links

1. W. Shieh, H. Bao, and Y. Tang, "Coherent optical OFDM: theory and design," *Opt. Express* **16**(2), 841–859 (2008).
2. J. Armstrong, "OFDM for optical communications," *J. Lightwave Technol.* **27**(3), 189–204 (2009).
3. X. Liu, F. Buchali, and R. W. Tkach, "Improving the nonlinear tolerance of polarization-division-multiplexed CO-OFDM in long-haul fiber transmission," *J. Lightwave Technol.* **27**(16), 3632–3640 (2009).
4. S. Chandrasekhar, X. Liu, B. Zhu, and D. W. Peckham, "Transmission of a 1.2-Tb/s 24-carrier no-guard-interval coherent OFDM superchannel over 7200-km of ultra-large-area fiber," in *Proceedings of European Conference on Optical Communications* (2009), paper PD 2.6.
5. A. Lowery and J. Armstrong, "Orthogonal-frequency-division multiplexing for dispersion compensation of long-haul optical systems," *Opt. Express* **14**(6), 2079–2084 (2006).
6. G. Bosco, A. Carena, V. Curri, P. Poggiolini, and F. Forghieri, "Performance limits of Nyquist-WDM and CO-OFDM in high-speed PM-QPSK systems," *IEEE Photonics Technol. Lett.* **22**(15), 1129–1131 (2010).
7. F. Chang, K. Onohara, and T. Mizuochi, "Forward error correction for 100 G transport networks," *IEEE Commun. Mag.* **48**(3), S48–S55 (2010).
8. X. Hong, X. Hong, and S. He, "Linearly interpolated sub-symbol optical phase noise suppression in CO-OFDM system," *Opt. Express* **23**(4), 4691–4702 (2015).
9. W. Ryan and S. Lin, *Channel Codes: Classical and Modern* (Cambridge University, 2009).
10. B. Liu, L. Zhang, X. Xin, and J. Yu, "Robust generalized filter bank multicarrier based optical access system with electrical polar coding," *IEEE Photonics J.* **8**(5), 1–7 (2016).
11. Z. Wu, J. K. Fischer, and B. Lankl, "Experimental investigation of polar code performance for coherent UD-WDM PONs," in *Proceedings of Optical Fiber Communication Conference* (Optical Society of America, 2015), paper Th3E.7.
12. E. Arıkan, "Channel polarization: A method for constructing capacity-achieving codes for symmetric binary-input memoryless channels," *IEEE Trans. Inf. Theory* **55**(7), 3051–3073 (2009).
13. I. Tal and A. Vardy, "How to construct polar codes," *IEEE Trans. Inf. Theory* **59**(10), 6562–6582 (2013).
14. Z. Ye, "Chinese firms gain ground in 5G battle," <http://www.globaltimes.cn/content/1019126.shtml>.
15. P. Trifonov, "Efficient design and decoding of polar codes," *IEEE Trans. Commun.* **60**(11), 3221–3227 (2012).
16. A. Bravo-Santos, "Polar codes for the Rayleigh fading channel," *IEEE Commun. Lett.* **17**(12), 2352–2355 (2013).
17. W. Shieh and I. B. Djordjevic, *OFDM for Optical Communications* (Academic, 2009).
18. M. Bi, S. Xiao, H. He, J. Li, L. Liu, and W. Hu, "Power budget improved symmetric 40-Gb/s long reach stacked WDM-OFDM-PON system based on single tunable optical filter," *IEEE Photonics J.* **6**(2), 1–8 (2014).
19. I. Tal and A. Vardy, "List decoding of polar codes," *IEEE Trans. Inf. Theory* **61**(5), 2213–2226 (2015).

20. W. Shieh, "Maximum-likelihood phase and channel estimation for coherent optical OFDM," *IEEE Photonics Technol. Lett.* **20**(8), 605–607 (2008).
21. I. B. Djordjevic, W. Ryan, and B. Vasic, *Coding for Optical Channels* (Springer Science & Business Media, 2010).
22. ITU-T Recommendation G.975.1, Appendix I.9 (2004).
23. B. Li, H. Shen, and D. Tse, "An adaptive successive cancellation list decoder for polar codes with cyclic redundancy check," *IEEE Commun. Lett.* **16**(12), 2044–2047 (2012).
24. J. Yang, C. Zhang, H. Zhou, and X. You, "Pipelined belief propagation polar decoders," in *Proceedings of IEEE International Symposium on Circuits and Systems* (IEEE, 2016), pp. 413–416.

1. Introduction

Recently, coherent optical orthogonal frequency division multiplexing (CO-OFDM) technique has been considered as a promising technique for future fiber-optic communication network, especially for long-haul transmission such as backbone network [1–3], due to the advantages of flexible bandwidth allocation, high spectral efficiency, robustness to chromatic dispersion and convenient impairment compensation with digital signal processing (DSP) brought by OFDM [2] and the advantages of superior receiver sensitivity, long repeater spacing, multiple modulation methods available and large communication capability brought by coherent detection [4]. To meet the demand of exponential growth in internet traffic, high-speed long-haul CO-OFDM system has been extensively studied [4–6]. However, there exists two main challenges. First, as the speed of long-haul transmission systems increases up to 25-Gb/s, 40-Gb/s and more, poor optical-signal-to-noise environment becomes more commonplace due to the deployment of more optical amplifiers [7]. Second, OFDM is quite susceptible to phase noise [8] which is mainly induced by laser linewidth and the accumulated dispersion over long-distance transmission, resulting in the system performance degradation. This phenomenon will be more severe in coherent system where two lasers must track one another. Thus the laser linewidth requirement will be strict, leading to the increase in system cost. The forward error correction (FEC) codes can play a critical role in long reach fiber-optic system by providing extra code gain in a cost-effective way [7]. Several FEC codes, such as concatenated code, low-density parity-check (LDPC) code, and Turbo code have been used in optical systems [9], where LDPC codes have become the most popular choice [10]. Since LDPC code may display error floor due to the iterative decoding, it is commonly concatenated with an outer algebraic code to suppress the error floor and resist burst error. However, the high complexity and large processing delay of such a concatenated scheme will restrict its application [11], thus non-concatenated FEC code is more preferred. The polar code, as a novel provable Shannon capacity-achieving code sequence with low encoding and decoding complexities [12], can get robust error correction with explicit construction and avoid the error floor problem [13] which makes it attractive for many applications, and it has been chosen by 3rd Generation Partnership Project (3GPP) as the control channel encoding scheme for the application of fifth-generation (5G) in the enhanced mobile broadband (eMBB) scenario recently [14]. Current researches of the polar code mainly focus on wireless/mobile communications [15,16], while for CO-OFDM system which needs transmission extension and performance improvement, polar code may also be a potential FEC option due to its robust error correct capability and low complexity [12,13].

To study the polar code in CO-OFDM scenario, whose quasi-static channel [17] is different from the wireless Rayleigh fading channel, in this paper, to the best of our knowledge, a novel polar coded CO-OFDM system is proposed and demonstrated experimentally for the first time. The results show that it achieves a net coding gain (NCG) of more than 10 dB at bit error rate (BER) of 10^{-3} over 25-Gb/s 480-km transmission in comparison with the conventional CO-OFDM system. Compared to LDPC coded case, the polar coded signal provides a NCG of 0.88 dB @BER = 10^{-3} over 160-km transmission. Moreover, the polar coded signal can relieve the laser linewidth requirement to get a more cost-effective system. The remainder of this paper is organized as follows. Section 2 demonstrates the principle of polar coded CO-OFDM theoretically. Section 3 investigates the

polar decoding method suitable for 25-Gb/s CO-OFDM system first, and then presents the BER performance of LDPC coded and polar coded systems to verify the potentiality of the proposed scheme for long-distance CO-OFDM system. At last, the laser linewidth tolerance is investigated to further reveal the advantage of polar code. Conclusions are given in section 4.

2. Principle of polar coded CO-OFDM

The schematic diagrams of M-quadrature amplitude modulation (M-QAM) polar coded CO-OFDM signal generation and post-processing procedures are illustrated in Figs. 1(a) and 1(b) respectively. As shown in Fig. 1(a), the user's binary sequence data U of length u is encoded with polar code [13] after serial to parallel conversion. Assuming that polar code is of length N ($N = 2^n$, n is a positive integer), the number of code unit is t ($t = u/N$). In each code unit, the output polar coded data is labeled as x_{mp-m+q} ($p = 1, 2, 3, \dots, N/m$, $q = 1, 2, 3, \dots, m$, $m = \log_2 M$),

$$x = U \cdot G_N = U \cdot B_N \cdot \begin{bmatrix} 1 & 0 \\ 1 & 1 \end{bmatrix}^{\otimes n} \quad (1)$$

where G_N is the generator matrix, B_N is the bit-reversal operation, $\otimes n$ denotes the n^{th} Kronecker power of the matrix. After polar encoding for t units, they are Gray mapping to the M-QAM constellation every m -bits as a group. To reduce the signal transmission power of high-order modulation, the power of M-QAM modulation is normalized. After M-QAM modulation, the sequence

$\underbrace{x_1, x_2, \dots, x_{N/m}}_1, \underbrace{x_{N/m+1}, x_{N/m+2}, \dots, x_{2N/m}}_2, \dots, \underbrace{x_{(t-1)N/m+1}, x_{(t-1)N/m+2}, \dots, x_{tN/m}}_t$ (t code units) is mapping to subcarriers in preparation for OFDM modulation. The frequency-domain signal in e -th subcarrier and f -th OFDM symbol is denoted by Z_{ef} ($e = 1, 2, 3, \dots, \text{Data}N$, $f = 1, 2, 3, \dots, N_s$). The total number of subcarriers is N_{sc} of which $\text{Data}N$ subcarriers carrying data ($e = Nul$ is the starting point of data subcarrier), the number of OFDM symbols is S . The M-QAM signal maps into the subcarriers in the order of $Z_{Nul+1,1}, Z_{Nul+2,1}, Z_{Nul+3,1}, \dots, Z_{Nul+\text{Data}N,1}, Z_{Nul+1,2}, Z_{Nul+2,2}, Z_{Nul+3,2}, \dots, Z_{Nul+\text{Data}N,2}, \dots, Z_{Nul+\text{Data}N,S}$. The subcarriers left are mapping with 0. Then pilot subcarriers are inserted for channel estimation and phase compensation at receiver. After inverse fast Fourier transform (IFFT) and adding cyclic prefix (CP), OFDM modulation is implemented. Meanwhile, the PN sequence is added for synchronization at receiver after parallel to serial conversion. In-phase (I) and quadrature (Q) components of the polar coded OFDM signal are transmitted separately. As shown in Fig. 1(b), the received I and Q signals filtered by low-pass filter (LPF) perform the OFDM symbol synchronization first. By serial to parallel conversion, removing CP, fast Fourier transform (FFT), channel estimation, phase compensation and subcarrier demapping [18], OFDM demodulation is completed. Then, M-QAM soft demodulation is carried out. Soft demodulation calculates the log-likelihood ratio (LLR) of each information bit [7]. Then LLR is used to choose the codeword with the minimum Euclidean distance in the following soft-decision decoding. Since the signal before M-QAM demodulation is of length $N \cdot t/m$, we take a sequence of length N/m , whose demodulation output will be the input of one decode unit in the subsequent polar decoder, as an example to detail the M-QAM soft demodulation in the next paragraph.

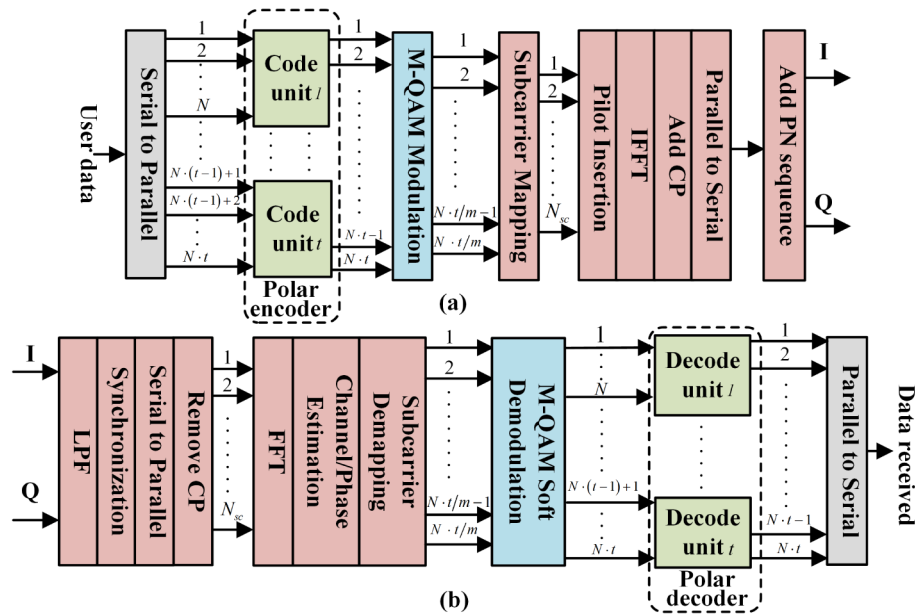


Fig. 1. Schematic diagrams of M-QAM polar coded CO-OFDM signal (a) generation and (b) post-processing.

The signal before M-QAM demodulation is labeled as $y_p = y_{p,Re} + i \cdot y_{p,Im}$. Assume $x_k^{q,0}$ is the demapping condition when $x_{mp-m+q} = 0 (k = 1, 2, 3 \dots, 2^{m-1}, p = 1, 2, 3 \dots, N/m, q = 1, 2, 3 \dots, m)$, $x_k^{q,0}$ can be expressed as $x_k^{q,0} = x_{k,Re}^{q,0} + i \cdot x_{k,Im}^{q,0}$ since it's a complex number. Thus the prior probability can be measured as

$$\begin{aligned}
 P(y_p | x_{mp-m+q} = 0) &= \sum_{k=1}^{2^{m-1}} P(y_{p,Re}, x_{k,Re}^{q,0}) \cdot P(y_{p,Im}, x_{k,Im}^{q,0}) \\
 &= \sum_{k=1}^{2^{m-1}} \frac{1}{\sigma\sqrt{2\pi}} \exp\left(-\frac{(y_{p,Re} - x_{k,Re}^{q,0})^2}{\sigma^2}\right) \cdot \frac{1}{\sigma\sqrt{2\pi}} \exp\left(-\frac{(y_{p,Im} - x_{k,Im}^{q,0})^2}{\sigma^2}\right) \quad (2)
 \end{aligned}$$

where σ is the standard deviation of noise. Similarly, $P(y_p | x_{mp-m+q} = 1)$ can be measured. Since 0 and 1 of the polar encoded sequence have the equal probability to appear,

$$P(x_{mp-m+q} = 0) = P(x_{mp-m+q} = 1) = \frac{1}{2} \quad (3)$$

Also, according to the characteristic of probability,

$$P(y_p) = P(y_p | x_{mp-m+q} = 0) \cdot P(x_{mp-m+q} = 0) + P(y_p | x_{mp-m+q} = 1) \cdot P(x_{mp-m+q} = 1) \quad (4)$$

Based on Eq. (3) and Eq. (4), the posterior probability can be expressed as

$$\begin{aligned}
 \Pr(x_{mp-m+q} = 0 | y_p) &= \frac{P(y_p | x_{mp-m+q} = 0) \cdot P(x_{mp-m+q} = 0)}{P(y_p)} = \frac{P(y_p | x_{mp-m+q} = 0)}{2P(y_p)} \\
 &= \frac{P(y_p | x_{mp-m+q} = 0)}{P(y_p | x_{mp-m+q} = 0) + P(y_p | x_{mp-m+q} = 1)} \quad (5)
 \end{aligned}$$

Similarly,

$$\Pr(x_{mp-m+q} = 1 | y_p) = \frac{P(y_p | x_{mp-m+q} = 1)}{P(y_p | x_{mp-m+q} = 0) + P(y_p | x_{mp-m+q} = 1)} \quad (6)$$

Equation (5) and Eq. (6) can be measured with the help of Eq. (2), which is based on the channel electrical signal-to-noise ratio (SNR) since the polar decoder simplifies the channel as additive white Gaussian noise (AWGN) channel [19].

The posterior probability distributions $\Pr(x_{mp-m+q} = 0 | y_p)$ and $\Pr(x_{mp-m+q} = 1 | y_p)$, as outputs of M-QAM demodulator, are input into one decode unit of the subsequent polar decoder [12,19]. At last, data is received after parallel to serial conversion.

3. Experiment setup and result analysis

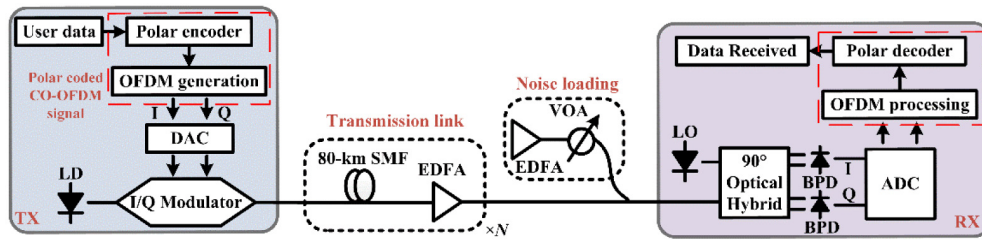


Fig. 2. Setup of the polar coded CO-OFDM system.

To verify the practical use of the polar coded CO-OFDM system, experiment was conducted following system architecture in Fig. 2. In the transmitter (TX), a continuous-wave laser (LD) at 1550 nm served as the light source. The output of the LD (Koheras AdjustiK-E15) passed through a polarization controller which was precisely adjusted before injecting into the in-phase/quadrature (I/Q) modulator (FUJITSU FTM7960EX) to get the best modulation performance. I and Q components of the polar coded OFDM signal were generated offline in MATLAB and loaded into the arbitrary wave generator (AWG) with 20-GS/S sampling rate. Two output channels of the AWG (Tektronix AWG7122C) were first amplified by the high linearity power amplifiers (Analog Devices Inc. ADL5240) respectively to mitigate the inherent unsatisfactory frequency response of AWG, and then drove the I/Q modulator biased at the null point to achieve a linear RF-to-optical conversion [1]. The output optical polar coded OFDM signal transmitted through the loop which comprises of 80-km standard single mode fiber (SMF) and an erbium doped fiber amplifier (EDFA). After fiber transmission, the output of an EDFA (WXZTE-WZEDFA) functioned as noise loading, with a variable optical attenuator (VOA) adjusting the SNR. In the receiver (RX), the received signal passed through a polarization controller first and then injected into a 90° optical hybrid (Kylia COH28-X), together with the local oscillator (LO) output. Four outputs of the hybrid were detected by a pair of BPDs (Discovery DSC-R412). The output electrical signals of BPDs were sampled by a real-time oscilloscope (LeCroy SDA 830Zi-A) and offline processed in MATLAB. The parameters of OFDM signal were as follows. The FFT size was 128 points of which 40 subcarriers were used for 16-QAM modulation. 10 subcarriers from the zero frequency were set to null subcarriers to mitigate the ground noise, so OFDM signal occupied the frequency from 780 MHz to 3.9 GHz which satisfies the working condition of the power amplifier with operating frequency from 100 MHz to 4 GHz. The cyclic prefix (CP) length was 16 (12.5%). The total number of measured symbols was 800. So the data rate of OFDM signal is 25-Gb/s. The polar code is of length $N = 512$ and code rate $R = 0.5$. The code unit t is set to be 250 according to OFDM signal.

First, to choose the polar decoding method suitable for 25-Gb/s CO-OFDM system, the successive cancellation (SC) decoder [12] and successive cancellation list (SCL) decoder [19] with different decoding list sizes (L) are analyzed. Taking 160-km (2-loop) CO-OFDM system for an example, the BER performance as a function of electrical SNR is presented in Fig. 3. Note that BER is calculated based on the Monte Carlo method. It can be seen that the performance of SCL decoder is much better than the SC decoder. As for SCL decoder, the system performance becomes better with the increasing decoding list size, however, the computational complexity will increase as well [19]. Since almost no BER difference between $L = 4$ and $L = 8$ is observed, the SCL decoder with list size 4 is the best choice.

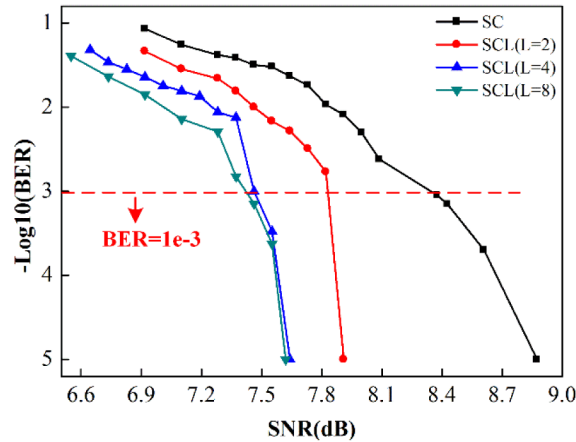


Fig. 3. BER performances with SC decoder and SCL decoder of different list sizes in 160-km 25-Gb/s polar coded CO-OFDM system.

Then, the experimental BER performance as a function of electrical SNR is presented in Fig. 4(a). Due to the limitations of experimental instruments in our lab, we only demonstrated the cases of transmission distance up to 160 km. To further demonstrate polar coded CO-OFDM system over longer transmission distance, we conducted the corresponding simulation which was established on the commercial simulation software OptiSystem 7.0 combined with MATLAB. To achieve the best fit with experimental results, all the parameter settings of system devices were set to the same as experimental setup. Note that laser linewidths in both TX and RX were set to be 0.01 MHz which was the same as the experimental laser. The fiber launching power is adjusted precisely for each transmission distance respectively to obtain the best performance. And to make a fair comparison, the launching powers for the same transmission distance with polar code and LDPC code are adjusted to the same. The noise model used in the simulation was Gaussian noise which was the same as the simplified noise model in the experiment [20] and the channel model used by polar decoder [19]. From the simulation results in Fig. 4(b) and the experiment results in Fig. 4(a), it can be seen that the simulation results are in good agreement with the experiment ones. The rightmost set of curves are the measured pre-FEC BERs, the leftmost set of curves are post-FEC BERs which drop off sharply. In Fig. 4(a), for 160-km polar coded transmission, no post-decoding error event is detected when SNR is larger than 7.64 dB and a NCG of 7.5 dB @BER = 10^{-3} is achieved in comparison with the pre-FEC curve. Note that NCG is the saving SNR required to achieve a given BER when coding is used compared to that with no coding [21]. In Fig. 4(b), for 320-km transmission aided by polar code, no post-decoding error event is detected when SNR is larger than 7.74 dB and a NCG of 10.2 dB @BER = 10^{-3} are obtained. There is barely BER performance difference between 160-km and 320-km transmissions which indicates that polar-coded CO-OFDM signal can bridge the performance gap among various transmission distances effectively. For 480-km case, BER performance of conventional CO-

OFDM shows error floor and cannot even reach the FEC threshold of $\text{BER} = 3.8 \times 10^{-3}$ [22], and the constellation diagrams of received signal and signal with channel/phase estimation, presented in insert (i) and (ii) of Fig. 4(b) respectively, are too bad to perform the subsequent QAM demodulation. However, with the help of polar code, no error event is detected when SNR is larger than 9.13 dB and a NCG of larger than 10 dB @ $\text{BER} = 10^{-3}$ is achieved. It indicates that the polar coded system can reduce the error floor massively and extend the maximum reachable transmission distance. Note that since the error floor of 480-km conventional CO-OFDM system reaches 1.5×10^{-2} , performance of transmission distance longer than 480 km isn't demonstrated. It can be seen that the post-FEC performance of 480-km transmission is different from the 160-km/320-km case, the reason can be explained as follows. The accumulated system noise and fiber dispersion can be simplified as AWGN model when the transmission distance is not long enough such as 160 km and 320 km since their effect on pre-FEC performance deterioration is small, while when the distance is long enough such as 480 km, they can't be simplified as AWGN since they worsen the pre-FEC performance so pronouncedly that BER error floor occurs. The noise model has some impact on the performance of FEC decoding because the polar decoder simplifies the channel as AWGN channel [19].

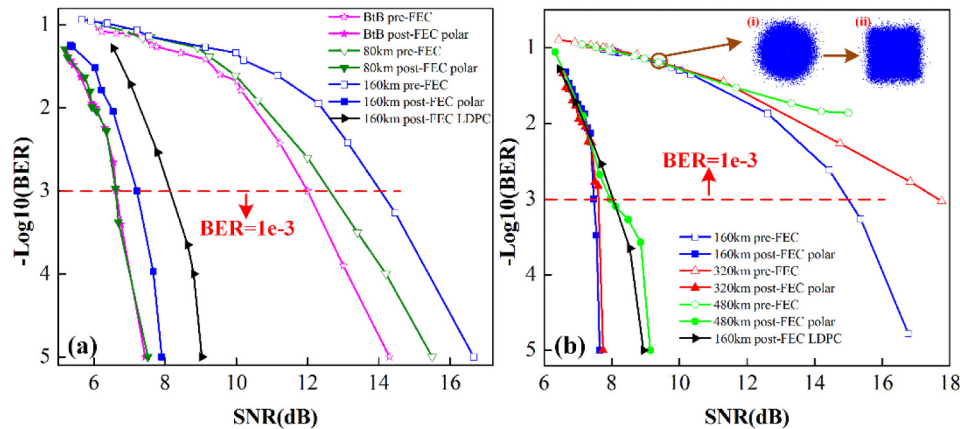


Fig. 4. (a) Experiment and (b) simulation results of BER versus electrical SNR in 25-Gb/s CO-OFDM system with polar code and LDPC code over different transmission distances.

Meanwhile, the performance of low-density parity-check (LDPC) coded 160-km system is also presented in Fig. 4. To make a fair comparison, the LDPC code of the same code length $N = 512$ and code rate $R = 0.5$ [23,24] as polar code is employed in both experiment and simulation. The LDPC encoder is based on a specified parity-check matrix and the classical belief propagation (BP) algorithm with 50 iterations is used in LDPC decoder. Compared to LDPC coded signal, polar coded signal provides NCGs of 0.88 dB @ $\text{BER} = 10^{-3}$ and around 2.23 dB @ $\text{BER} = 10^{-9}$ in theory. In conclusion, the polar code achieves excellent error correction performance which is more remarkable in longer transmission distance. Moreover, the computing complexities for polar encoder and decoder are $O(N \log N)$ and $O(L \log N)$ respectively [19], while the computing complexities for LDPC encoder and decoder are $O(N^2)$ and $O(\alpha N)$ respectively where α is the number of iterations, revealing the low complexity of polar code [10,12,13,19]. Therefore, polar code is suitable for CO-OFDM system whose applications need performance improvement and transmission distance extension.

To further reveal the advantage of the polar code used in CO-OFDM system, the laser linewidth tolerance is discussed by simulation because one disadvantage of CO-OFDM is that the laser linewidth requirement is far more stringent than direct detection optical OFDM.

Figure 5 shows the receiver power penalty as a function of laser linewidth over different transmission distances. Note that the laser linewidths in both TX and RX are set to be the same. The power penalty is defined as the decrease in receiver sensitivity at BER of 3.8×10^{-3} compared to the situation when ideal laser, i.e., 0-MHz linewidth laser, is used for each case. For a fixed power penalty of 2 dB, the linewidth requirement is 0.5 MHz and 0.1 MHz in 160-km and 320-km transmission respectively for conventional OFDM signal. Since OFDM without polar code over 480-km transmission cannot reach the BER of 3.8×10^{-3} , its result isn't presented. However, for polar coded signal, the linewidth requirement is >3 MHz, 2.2 MHz and 1.4 MHz for 160-km, 320-km and 480-km transmission respectively. It can be seen that the use of polar code can make CO-OFDM system robust to laser linewidth which is more obviously over longer transmission distance. Therefore, aided by polar code, laser linewidth requirement will be less strict and CO-OFDM system can become more cost-effective.

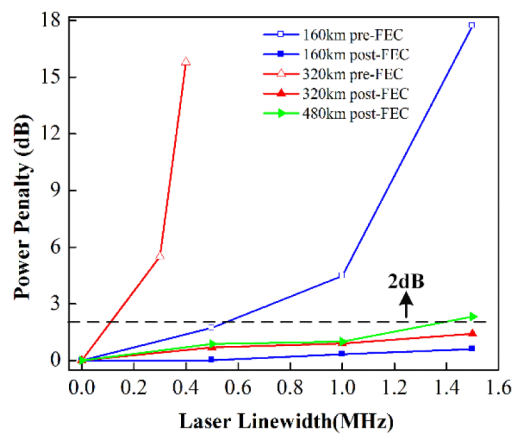


Fig. 5. Receiver power penalty @BER = 3.8×10^{-3} versus laser linewidth in 25-Gb/s polar coded CO-OFDM system over different transmission distances.

4. Conclusion

In this paper, for the first time, a novel polar coded 25-Gb/s CO-OFDM system is proposed and demonstrated by experiment, employing the SCL decoder with list size 4. Results show that at BER of 10^{-3} , the polar coded CO-OFDM obtains NCGs of more than 10 dB over 480-km transmission compared to conventional CO-OFDM and 0.88 dB over 160-km transmission compared to LDPC coded case. Moreover, polar coded signal relieves the laser linewidth requirement from 0.5 MHz to larger than 3 MHz, from 0.1 MHz to 2.2 MHz over 160-km and 320-km transmissions respectively for a power penalty of 2 dB @BER = 3.8×10^{-3} . This paper verifies that the polar code can provide significant system performance improvement and cost reduction for CO-OFDM system with simple structure and low complexity, which may become a potential choice for its FEC option.

Funding

National Natural Science Foundation of China (NSFC) (61271216, 61501157, 61221001, 61090393 and 61433009); National 973 Program of China (2010CB328205, 2010CB328204 and 2012CB315602); Natural Science Foundation of Zhejiang Province (LQ16F050004).